International Journal of Heat and Mass Transfer 54 (2011) 5020–5029

Contents lists available at ScienceDirect

International Journal of Heat and Mass Transfer

journal homepage: www.elsevier.com/locate/ijhmt

Effect of thermal conductivity and thickness of the walls in the convection of a viscoelastic Maxwell fluid layer

I. Pérez-Reyes *, L.A. Dávalos-Orozco

Instituto de Investigaciones en Materiales, Departamento de Polímeros, Universidad Nacional Autónoma de México, Ciudad Universitaria, Circuito Exterior S/N, Delegación Coyoacán, 04510 México D.F., Mexico

ARTICLE INFO

Article history:
Received 21 October 2010
Received in revised form 5 July 2011
Accepted 5 July 2011
Available online 9 August 2011

Keywords:
Convection
Viscoelastic fluid
Thermal conductivity
Wall thickness

ABSTRACT

Results for the linear thermoconvective stability of a layer of viscoelastic Maxwell fluid are presented. The stability problem is characterized by taking into account the lower and upper wall thermal conductivities as well as their thicknesses. This allows more realistic theoretical boundary conditions. A system consisting of a horizontal infinite Maxwell fluid layer confined between two parallel walls perpendicular to gravity is considered. The critical Rayleigh number R_c, the frequency of oscillation ω_c and the wavenumber k_c were determined for fixed values of the relaxation time constant F and the Prandtl number Pr. The results are given for a range of wall thermal conductivities and thicknesses. Analytical and numerical solutions were calculated. Some unexpected results were found in comparison to those of the Newtonian fluid where the criticality curves become more unstable when the conductivities of the walls change from very good conductors to very bad conductors.

1. Introduction

Thermal convection of viscoelastic fluids may occur in many experimental set-ups and technological applications such as material processing, food and chemical industries. A particular area of research of growing interest where hydrodynamics of viscoelastic fluids is involved is that of the flow properties of biomolecules. In manipulation of biomolecules like DNA, for genome analysis and other applications, problems related to hydrodynamics arise and the theory of viscoelastic fluids can be used. Some efforts on this matter have been done since many years ago such as that of Bowen and Zimm [1] who determine some viscoelastic properties of DNA.

Thermal convection appearing in aqueous suspensions of DNA which behave as viscoelastic fluids (see [2] for example) is a very complex subject. This is due to a number of physical mechanisms that contribute or compete to set in convective cells in the suspension. Krishnan et al. [3] developed a device where Rayleigh convection is relevant to perform thermally activated chemical reactions such as polymerase chain reaction (PCR). In this case Krishnan et al. [3] proposed to replace the conventional thermocyclers by Rayleigh convection cells that make the device very simple and of easily assembly in any laboratory. Braun and Libchaber [4] proposed an efficient mechanism for trapping DNA in solution through the interaction of thermophoresis and thermoconvection. A study of the PCR in thermal convection for replication of DNA was conducted by Braun et al. [5] and by Braun [6]. In a more recent paper the interaction of thermophoresis and thermoconvection have been studied along with PCR for replication of DNA by Mast and Braun [7]. Theoretical advances on the hydrodynamics of this suspensions which exhibit viscoelastic behavior have been conducted by Sri Krishna [8] and Laroze et al. [9,10].

The aim of this paper is to study how the thermal properties and geometrical nature of the walls influence the hydrodynamic stability of a viscoelastic Maxwell fluid layer. The scenario we propose here has not been considered nor discussed before. The theory developed in this work may be significant to complement and understand the phenomena appearing in the applications.

The linear thermoconvective stability of a viscoelastic Maxwell fluid layer heated from below is investigated. The constitutive equation for the Maxwell fluid is used. It has a relaxation time that, when large, allows for important elastic properties. The physical problem investigated here is to understand the effect the thermal conductivity and thickness of the walls has on the instability. In the case of natural convection in a Newtonian fluid, this influence was investigated by Metcalfe and Behringer [11], Cerisier et al. [12] and Howle [13].

Natural convection in viscoelastic Maxwell fluids was first investigated by Vest and Arpaci [14] and in an Oldroyd fluid layer by Takashima [15]. In both papers, the temperature boundary conditions are of fixed temperature at the walls.

* Corresponding author.
E-mail addresses: ildebrando3@gmail.com (I. Pérez-Reyes), ldavalos@servidor.unam.mx (L.A. Dávalos-Orozco).

0017-9310/$ - see front matter © 2011 Elsevier Ltd. All rights reserved.
doi:10.1016/j.ijheatmasstransfer.2011.07.016

Nomenclature

D_L	ratio of thicknesses (lower wall/fluid)
D_U	ratio of thicknesses (upper wall/fluid)
d_F	depth of fluid layer
d_L	thickness of lower wall
d_U	thickness of upper wall
F	relaxation time
g	acceleration due to gravity
K_L	thermal conductivity of the lower wall
K_F	thermal conductivity of the fluid
K_U	thermal conductivity of the upper wall
k	wavenumber
Pr	Prandtl number
R	Rayleigh number
T_F^*	dimensional fluid temperature profile
T_L^*	dimensional lower wall temperature profile
T_U^*	dimensional upper wall temperature profile
T_F	dimensionless fluid temperature profile
T_L	dimensionless lower wall temperature profile
T_U	dimensionless upper wall temperature profile
T_{BL}	temperature below the lower wall
T_{AU}	temperature above the upper wall
w	velocity perturbation
X_L	ratio of thermal conductivities (fluid/lower wall)
X_U	ratio of thermal conductivities (fluid/upper wall)
z^*	dimensional vertical coordinate
z	dimensionless vertical coordinate

Greek symbols

α	volumetric expansion coefficient of the fluid
θ	temperature perturbation
λ	relaxation time, s
κ	thermal diffusivity of the fluid, $cm^2\ s^{-1}$
ν	kinematic viscosity, $cm^2\ s^{-1}$
ρ	fluid density, $g\ cm^{-3}$
ω	frequency of oscillation

Subscripts

c	critical value
L	lower
U	upper

The fixed heat flux boundary condition at the walls was investigated by Kolkka and Ierley [16] for natural convection of a viscoelastic Oldroyd fluid layer heated from below. Martínez-Mardones and Pérez-García [17] reported results for the stationary and oscillatory convection and a codimension-two point for the case of fixed temperature at the walls. Several advances in the study of convection in viscoelastic fluids have been made by Rosenblat [18], Park and Lee [19,20], Martínez–Mardones et al. [21], Dávalos-Orozco and Vázquez Luis [22], Martínez–Mardones et al. [23–26] and more recently by Li and Khayat [27]. Some other advances in coupled buoyancy and capillary thermoconvection in viscoelastic fluids have also been made by Dauby et al. [28], Lebon et al. [29] and Parmentier et al. [30]; and earlier for capillary thermoconvection alone by Getachew and Rosenblat [31].

The system consists of a horizontal fluid layer between two parallel walls which are perpendicular to gravity. The system is characterized by nondimensional parameters such as: the Rayleigh number R, the Prandtl number Pr, the relaxation time constant F, the thermal conductivity ratios of the fluid to the lower and upper walls (X_L, X_U), the thickness ratios of the lower and upper walls respect to that of the fluid layer (D_L, D_U), the frequency of oscillation ω and the perturbation wavenumber k. The results presented here are of great importance because the physical and geometrical properties of the walls are taken into account. This allows the theory to better simulate the real experimental conditions.

The paper is organized as follows. In Section 2 the formulation of the problem is given including the governing equations, boundary conditions as well as nondimensional parameters of the problem. In Section 3 a solution to the eigenvalue problem using analytical techniques and numerical methods is presented. Finally, a discussion of the results is presented in the last section.

2. Formulation of the problem

Consider the natural convection in a viscoelastic Maxwell fluid layer confined between two infinite horizontal walls perpendicular to gravity. The lower and upper walls have thicknesses (d_L, d_U) and thermal conductivities (K_L, K_U), respectively. The upper surface of the lower wall and lower surface of the upper wall are located at $z = 0$ and $z = 1$, respectively. The fluid layer has density ρ, dynamic viscosity $\rho\nu$ (with ν being the kinematic viscosity), thermal conductivity K_F and thickness d_F.

The equations of momentum and energy of the incompressible Maxwell fluid are linearized and perturbed (see [14,15]). Next, the rotational operation is taken twice in the momentum equation to obtain the following system of coupled equations for the perturbations

$$\left(1 + F\frac{\partial}{\partial t}\right)\left(\frac{1}{Pr}\frac{\partial}{\partial t}\nabla^2 w - R\nabla_\perp^2\theta\right) = \nabla^4 w \tag{1}$$

$$\left(\frac{\partial}{\partial t} - \nabla^2\right)\theta = w \tag{2}$$

where w is the fluid velocity and θ is the temperature. The dimensionless parameters in Eqs. (1) and (2) are $F = \lambda\kappa/d_F^2$ the relaxation time, $Pr = \nu/\kappa$ the Prandtl number and $R = \alpha g d_F^3 (T_{BL} - T_{AU})/[\nu\kappa(1 + D_U X_U + D_L X_L)]$ the Rayleigh number. Dimensionless variables are obtained by using the following scales: d_F for length, d_F^2/κ for time, $(T_{BL} - T_{AU})/(1 + D_U X_U + D_L X_L)$ for temperature and κ/d_F for velocity. Notice that $T_{BL} > T_{AU}$.

In the basic state there is no motion in the fluid and the heat transport is only by conduction. Before perturbation, the main temperature profiles for the fluid and walls are calculated from the linear stationary heat diffusion equation $d^2T/dz^{*2} = 0$. These dimensional solutions satisfy the following thermal boundary conditions. The temperature is constant over the outer surface of each wall, that is, $T_L^* = T_{BL}$ at $z^* = -d_L$ and $T_U^* = T_{AU}$ at $z^* = d_F + d_U$. They satisfy the continuity of temperature and heat flux at the interface of the fluid with each wall at $z^* = 0$ and d_F, respectively. The solutions, in dimensional form, are:

$$T_F^* = -\frac{(T_{BL} - T_{AU})z^*}{d_F(1 + D_U X_U + D_L X_L)} + T_{BL} - \frac{(T_{BL} - T_{AU})D_L X_L}{(1 + D_U X_U + D_L X_L)} \tag{3}$$

$$T_L^* = -\frac{(T_{BL} - T_{AU})X_L z^*}{d_F(1 + D_U X_U + D_L X_L)} + T_{BL} - \frac{(T_{BL} - T_{AU})D_L X_L}{(1 + D_U X_U + D_L X_L)} \tag{4}$$

$$T_U^* = -\frac{(T_{BL} - T_{AU})X_U z^*}{d_F(1 + D_U X_U + D_L X_L)} + T_{BL} - \frac{(T_{BL} - T_{AU})(1 + D_L X_L - X_U)}{(1 + D_U X_U + D_L X_L)} \tag{5}$$

Lets assume that $T_i = (T_i^* - T_{AU})(1 + D_U X_U + D_L X_L)/(T_{BL} - T_{AU})$, where the subscript i stands for (F, L, U). Then, in nondimensional form they can be rewritten as

$$T_F = -z + 1 + X_U D_U \tag{6}$$
$$T_L = -X_L z + 1 + X_U D_U \tag{7}$$
$$T_U = X_U(-z + 1 + D_U) \tag{8}$$

For the perturbed governing equations a normal modes separation in the form of $[w,\theta] = [W(z),\Theta(z)]\exp[i(k_x x + k_y y) + \sigma t]$ is considered. k_x and k_y are the x and y-components of the wavenumber vector with magnitude $k = \sqrt{k_x^2 + k_y^2}$. σ is a complex parameter whose real part σ_R and imaginary part ω are the growth rate and the frequency of oscillation, respectively. Thus after substitution in Eqs. (1) and (2) we obtain

$$(1 + F\sigma)\left[\frac{\sigma}{Pr}\left(\frac{d^2}{dz^2} - k^2\right)W - Rk^2\Theta\right] = \left(\frac{d^2}{dz^2} - k^2\right)^2 W \tag{9}$$

$$\left[\sigma - \left(\frac{d^2}{dz^2} - k^2\right)\right]\Theta = W \tag{10}$$

Dimensionless boundary conditions including the properties of the walls (see [12] for example) are

$$\begin{aligned} &W = DW = 0 \quad \text{at } z = 0, 1 \\ &\left(\frac{d}{dz} - \frac{q}{X_L \tanh qD_L}\right)\Theta = 0 \quad \text{at } z = 0 \\ &\left(\frac{d}{dz} + \frac{q}{X_U \tanh qD_U}\right)\Theta = 0 \quad \text{at } z = 1 \end{aligned} \tag{11}$$

where $q = \sqrt{k^2 + \sigma}$.

3. Analytical and numerical solutions

In this section the conditions for the onset of convection are determined by using the analytical Galerkin method (see [32] for more details) to solve the eigenvalue problem posed in the system of Eqs. (9) and (10) subject to the boundary conditions Eq. (11). Although this is an approximate method, it has very high precision. Besides, it gives the possibility to obtain an analytical expression for the Rayleigh number R. Consider the following expansion of W which already satisfies the boundary conditions

$$W = \sum_{n=0}^{\infty} A_n [z(z-1)]^{2+n} \tag{12}$$

Now, if the proposed expansion of Θ is

$$\Theta = \sum_{n=0}^{\infty} A_n \Theta_n \tag{13}$$

then, after substitution of W of Eq. (12) and Θ of Eq. (13) into Eq. (10), Θ_n is the solution of the following differential equation

$$\left[\sigma - \left(\frac{d^2}{dz^2} - k^2\right)\right]\Theta_n = [z(z-1)]^{2+n} \tag{14}$$

subjected to proper boundary conditions as given in Eq. (11). In this way by solving the differential equation Eq. (14) Θ_n can be easily calculated. Θ_n is not shown here and can be obtained from the authors upon request. Next, Eq. (9) is multiplied by W and integrated in the range $z = 0$ to $z = 1$, to get

$$0 = \left| \int_0^1 W_m \left(\frac{d^2}{dz^2} - k^2\right)\left[\frac{\sigma}{Pr}(1 + F\sigma) - \left(\frac{d^2}{dz^2} - k^2\right)\right] W_n \, dz - \left(1 + F\sigma\right)Rk^2 \int_0^1 W_m \Theta_n \, dz \right| \tag{15}$$

where use of Eqs. (12) and (13) have been made as well as some simplifications. Determinant Eq. (15) calculated with help of the software Maple, is the solvability condition from which the eigenvalue R is computed. The first approximation of R, corresponding to the element (0,0) of the matrix in the determinant Eq. (15), can be easily calculated. From here on, it is supposed that the walls have the same properties and geometry, that is $X_L = X_U = X$ and $D_L = D_U = D$. Then the result is:

$$R = \frac{q^{11}\coth q\left[\left(q^2 + B^2\right)\tanh q + 2qB\right]\left[C_1 + (1 + F\sigma)\left(k^2 + 12\right)\sigma Pr^{-1}\right]}{k^2(1 + F\sigma)\left(C_2 B^2 + C_3 B + C_4\right)} \tag{16}$$

where

$$\begin{aligned} B &= \frac{q}{X \tanh qD} \\ C_1 &= k^4 + 24k^2 + 504 \\ C_2 &= q(q^8 - 12q^6 + 504q^4 + 30240q^2 + 362880) \\ &\quad - 5040 \tanh\frac{q}{2}(q^2 + 12)^2 \\ C_3 &= 2q^6(q^4 - 12q^2 + 504)\coth q + 60480q^2(q^2 + 12)\operatorname{csch} q \\ &\quad - 5040q(q^2 - 6q + 12)(q^2 + 6q + 12) \\ C_4 &= q^3(q^8 - 12q^6 + 504q^4 - 30240q^2 - 362880) \\ &\quad + 181440q^4 \coth\frac{q}{2} \end{aligned}$$

The Rayleigh number given in Eq. (16) is a result that have not been reported before which includes k, X and D, without any restriction in their magnitudes. A second order estimate of R obtained from Eq. (15) was performed numerically.

The critical values for the Rayleigh number R_c, the wavenumber k_c and the frequency of oscillation ω_c were obtained as follows. The Rayleigh number in Eq. (16) is complex and the frequency which makes the imaginary part of R zero is used in the real part to calculate the marginal R for given D, X, Pr, F and k. In this way, k is varied until a minimum of R is found which is called the critical value R_c with corresponding k_c and ω_c. Notice from Eq. (16), that q is the argument of hyperbolic functions and, as explained above, it has the form $q = \sqrt{k^2 + \sigma}$. Therefore, it is not possible to give an explicit solution of the frequency of oscillation from the imaginary part of R in Eq. (16).

Results obtained by the Galerkin method were verified with a shooting numerical method and the agreement is very good. In order to apply this method, the Eqs. (9) and (10), subject to the boundary conditions Eq. (11) were integrated by a Runge–Kutta method while the resulting eigenvalue problem for R was solved by shooting various trials to satisfy the boundary conditions at $z = 1$. For given D, X, Pr, F and k, the R and ω which make zero the real and imaginary parts of a complex determinant of the trials are the marginal eigenvalues [33].

It is possible to obtain an expression of R in Eq. (16) in the limit of $X \to 0$, which corresponds to the fixed temperature boundary condition. In this limit only the term corresponding to B^2 will survive. Therefore, the equation becomes:

$$R = \frac{q^{11}[C_1 + (1 + F\sigma)(k^2 + 12)\sigma Pr^{-1}]}{k^2(1 + F\sigma)C_2} \tag{17}$$

When $F = 0$ the newtonian case is recovered and the frequency is zero. The limit $Pr \to 0$ can not be taken because it is a singularity corresponding to viscosity zero (inviscid limit). However, the limit $Pr \to \infty$ gives another expression for the Rayleigh number. That is:

$$R = \frac{q^{11}\coth q[(q^2 + B^2)\tanh q + 2qB]C_1}{k^2(1 + F\sigma)(C_2 B^2 + C_3 B + C_4)} \tag{18}$$

By considering the fixed temperature boundary condition at both walls, in the limit of small X, it was possible to compare the

critical values R_c, k_c and ω_c for fixed values of F with those reported by Vest and Arpaci [14] in their Table I, Takashima [15] in his Table I, Sokolov and Tanner [34] in their Table I and Martínez-Mardones and Pérez-García [17] in their Fig. 5. The agreement was very good. On the other hand, assuming the fixed heat flux boundary condition at both walls, in the limit of large X, the critical values R_c, k_c and ω_c for fixed values of F were also compared with those reported by Kolkka and Ierley [16] in their Tables I and II. In this case too, the agreement was excellent.

For fixed $Pr = 1$ curves of R_c, k_c and ω_c against X in the two limiting cases of small $D = 0.1$ and large $D = 100$ are shown in Fig. 1(a)–(c) for $F = 0.1$ and in Fig. 1(d)–(f) for $F = 100$, respectively. Notice that the curves corresponding to $D < 0.1$ are very near to that of $D = 0.1$. The same can be said for the curves corresponding to $D > 100$. It can be seen in Fig. 1(a) that for $Pr = 1$ and $F = 0.1$ a competition exists between oscillatory and stationary convection to destabilize the system. The change from oscillatory to stationary convection, at the codimension two point as stated by Martínez-Mardones and Pérez-García [17], appears at intermediate values in the range of X. This very interesting result shows that at $Pr = 1$ the convection can be stationary and the viscoelastic Maxwell fluid behaves as Newtonian. The competition between these two modes comes to an end at approximately $Pr = 1.4$ when convective motions set in only as oscillatory, as shown in Fig. 3. After the codimension two point the stationary convection destabilizes with X monotonically and the results agree with those of Cerisier et al. [12]. In the limit of fixed temperature boundary condition ($X \ll 1$) at both walls the following critical values were found: $R_c = 870.5590$, $k_c = 4.92$ and $\omega_c = 15.09$ [14,15,34]; while in the limit of fixed heat flux boundary condition ($X \gg 1$) at both walls it was found: $R_c = 720.0183$, $k_c = 0.02$ and zero frequency ω_c [12]. The codimension two points for $D = 0.1$ and $D = 100$ are located approximately

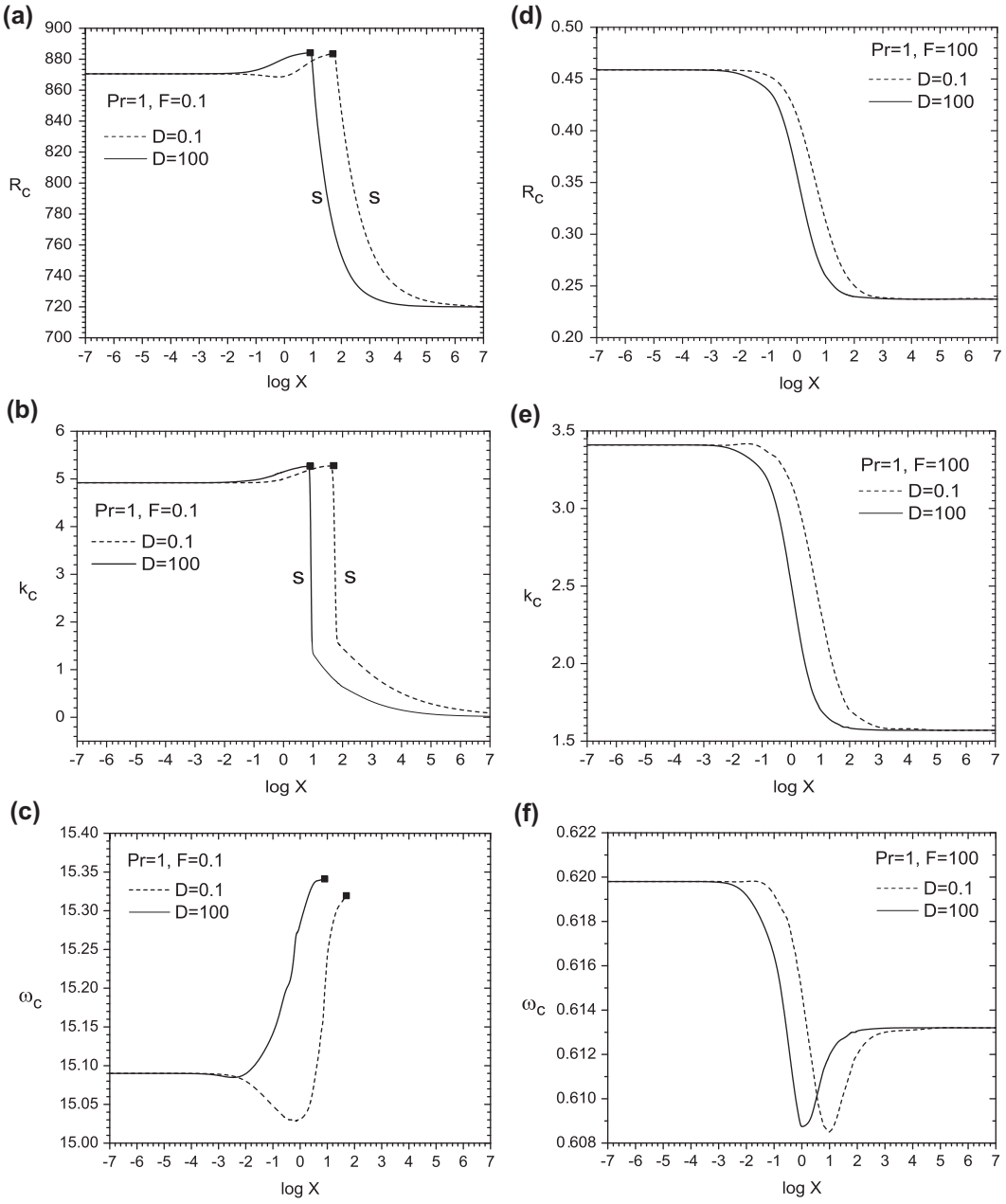

Fig. 1. Curves for $F = 0.1$: (a) R_c, (b) k_c and (c) ω_c against X, and curves for $F = 100$: (d) R_c, (e) k_c and (f) ω_c against X. Here, $Pr = 1$, $D = 0.1$ are indicated by dashed lines and $D = 100$ by continued lines.

at $X = 50$ and $X = 8$, respectively. An unexpected behavior was found in the curves of ω_c against X for $F = 0.1$ and $F = 100$ shown in Fig. 1(c) and (f). That is, besides the relative minimum that the ω_c has at the limit of fixed heat flux boundary condition, there is an absolute minimum at an intermediate value of X. We checked the curves for different values of Pr and found that this absolute minimum disappears only as Pr reaches $Pr = 10$. These results obtained by the Galerkin method were confirmed with the shooting method as well. For $Pr = 1$ and $F = 100$ in the limit of fixed temperature boundary condition at both walls the following critical values were found: $R_c = 0.4589$, $k_c = 3.41$ and $\omega_c = 0.6198$ [14,15,34]; while in the limit of fixed heat flux boundary condition at both walls it was found: $R_c = 0.2372$, $k_c = 1.57$ and $\omega_c = 0.6132$ [16]. The curves in Fig. 1(d) for $F = 100$ show that the system becomes more unstable as X increases and that in this case convective motions are only oscillatory.

For fixed $Pr = 10$ curves of R_c, k_c and ω_c against X in the two limiting cases of small $D = 0.1$ and large $D = 100$ are shown in Fig. 2(a)–(c) for $F = 0.1$ and in Fig. 2(d)–(f) for $F = 100$, respectively. For the case of $Pr = 10$ and $F = 0.1$ the value of (R_c, k_c, ω_c) increases with X. Here X has a stabilizing effect. Notice that this behavior is in contrast with that of the curves in the previous figures and in the next one. In Fig. 1(a) the stabilizing effect is incipient before the codimension two point appears. In the limit of fixed temperature boundary condition at both walls the following critical values were found: $R_c = 226.7151$, $k_c = 7.26$ and $\omega_c = 76.2593$ [14,15,34]; while in the limit of fixed heat flux boundary condition at both walls it was found: $R_c = 233.7246$, $k_c = 7.61$ and $\omega_c = 79.1547$ [16]. For the case of $Pr = 10$ and $F = 100$ the value of (R_c, k_c, ω_c) decreases with X. In the limit of fixed temperature boundary condition at both walls the following critical values were found: $R_c = 4.6230 \times 10^{-2}$, $k_c = 3.44$ and $\omega_c = 1.9625$ [14,15,34]; while in

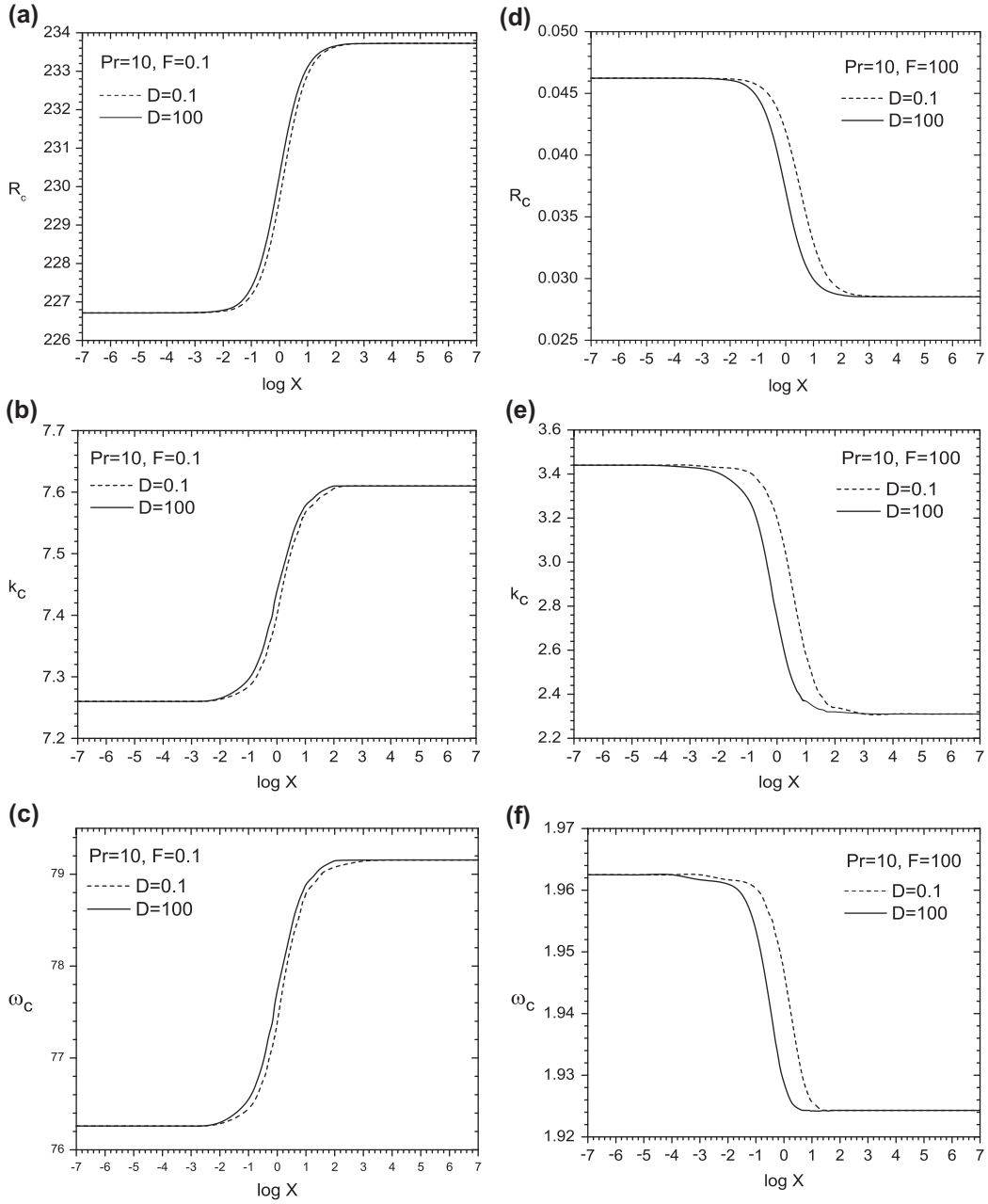

Fig. 2. Curves for $F = 0.1$: (a) R_c, (b) k_c and (c) ω_c against X, and curves for $F = 100$: (d) R_c, (e) k_c and (f) ω_c against X. Here, $Pr = 10$, $D = 0.1$ are indicated by dashed lines and $D = 100$ by continued lines.

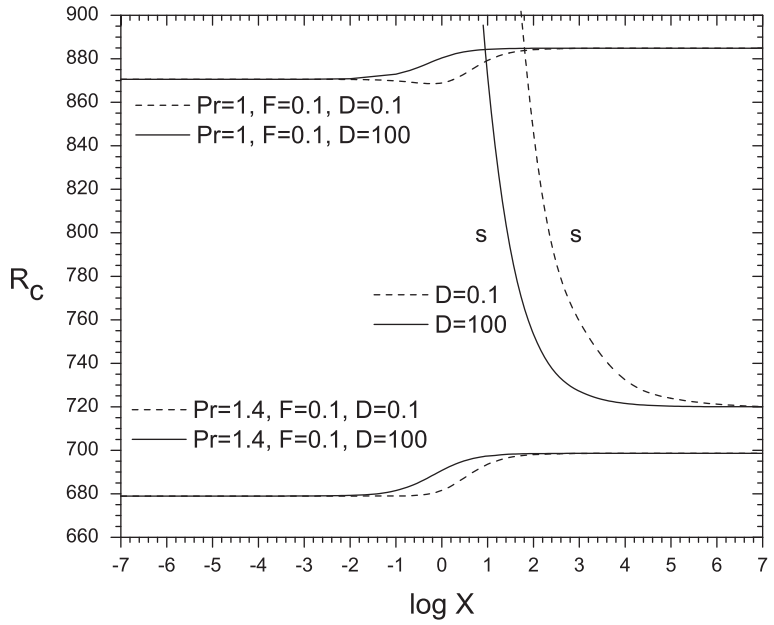

Fig. 3. Curves of R_c against X for fixed $F = 0.1$. Curves for $Pr = 1$ and $Pr = 1.4$ correspond to oscillatory convection and curves without Pr indicated correspond to stationary convection. Dashed line indicates $D = 0.1$ and continued line indicates $D = 100$.

the limit of fixed heat flux boundary condition at both walls it was found: $R_c = 2.8520 \times 10^{-2}$, $k_c = 2.31$ and $\omega_c = 1.9243$ [16].

A more explicit and clear presentation of the competition between stationary and oscillatory convection given in Fig. 1(a) is shown in Fig. 3. In the curves corresponding to oscillatory convection presented in Fig. 3 the elastic parameter is $F = 0.1$. There, the two pairs of curves of criticality for $Pr = 1$ and $Pr = 1.4$ correspond to oscillatory convection while the other two curves correspond to stationary convection. Notice that the codimension two points arising for $Pr = 1$ and different D's, disappear as Pr increases from $Pr = 1$ to approximately $Pr = 1.4$.

On the other hand note that for decreasing values of Pr convective motions set in first as oscillatory when X is small and they set in first as stationary when X is large. It has also been found, numerically, that if F increases then ω decreases suggesting that there is a balance between these two parameters.

It should be noted from Figs. 1 and 2 that in the limiting cases of small and large X both curves of $D = 0.1$ and $D = 100$ for R_c, k_c and ω_c collapse into one curve, as expected. This means that, also for the viscoelastic fluid (see [12]) the thickness of the walls have no influence on the onset of convection in these regions of X [14,15,34,17,16]. Notice that not always R_c approaches the value of 720 when $X \to \infty$ (see [35–37]). This means that even with the fixed heat flux boundary condition at the walls, stationary convection not always can occur in a viscoelastic Maxwell fluid [16], and under certain conditions, the convective motions can set in as oscillatory convection. The separation between every pair of curves at moderate values of X in Figs. 1 and 2 is clearly the effect of the difference between $D = 0.1$ and $D = 100$. In that region the thickness of the walls has important influence on the instability.

Curves presented in Figs. 1 and 2 show the role played by X. They show how X bridges the two limiting cases already studied since many years ago: perfect conducting walls and perfect insulating walls. It have been found in this study that for fixed Pr and growing X, convection cells appear faster in the fluid layer when $F = 0.1$ than when $F = 100$. The influence of the geometrical nature of the walls is noticeable across all the curves shown in Figs. 1 and 2 although this effect is magnified for the curves corresponding to ($Pr = 1$,$F = 0.1$) and ($Pr = 10$,$F = 0.1$).

It is of interest to give asymptotic solutions of R and ω of the convection problem to compare with the above given numerical results. These approximations were done using a Galerkin approach different from that of Chandrasekhar. The procedure is explained in Appendix A. Appendixes B and C show the results of asymptotic calculations based on the results of the Galerkin method presented in Appendix A. There, it can be found different asymptotic approximations as for $Pr \to \infty$, $F \to 0$, $F \to \infty$ and for two different limits of $D \to 0$ and $D \to \infty$. The approximate results for R and ω agree very well with the numerical calculations in their respective limit of approximation.

4. Conclusions

Very interesting results were found when the effects of the thermal conductivities and thicknesses of the bounding walls were taken into account in the convection of a viscoelastic Maxwell fluid. The case considered here is that of a system having walls with the same properties and geometry. The Prandtl numbers considered were $Pr = 1$, 10 and two representative wall relaxation times were taken into account, that is, $F = 0.1$, 100.

In the case of $Pr = 1$, it was shown that, in both cases of $F = 0.1$ and $F = 100$, the ratio of thermal conductivities X destabilizes the system. Notice that the effect of the thickness of the wall is more important here when $F = 0.1$ than when $F = 100$. A very interesting situation occurs at $F = 0.1$ due to the competition between stationary and oscillatory convection. This last interesting situation can be observed in Fig. 1(c) in the curves of ω_c vs. X when ω_c drops to zero when X increases; and in Fig. 3 where it is shown that oscillatory motions dominate the instability of the system as Pr increases to approximately $Pr = 1.4$. At the codimension two points, corresponding to different values of D, the convection becomes stationary. This is shown in the curves of Fig. 1(a) for R_c vs. X, as a sudden drop of the critical Rayleigh number, and a similar behavior is observed in the curves for k_c vs. X of Fig. 1(b) as well.

When $Pr = 10$ and $F = 0.1$ the relative effect of the thickness of the wall is reduced considerably. When $F = 100$ the magnitudes of the critical values are so small that it is difficult to notice an

important effect of the thickness of the walls. It was found that, depending on the value of the relaxation time F, the ratio of thermal conductivities X plays a different role. When F is small X stabilizes and when F is large X destabilizes.

These results are in contrast with those for stationary convection in a Newtonian fluid [11,12] where the system becomes more unstable when X increases.

Acknowledgments

The authors thank, Joaquín Morales, Cain González, Raúl Reyes, Ma. Teresa Vázquez and Oralia Jiménez for technical support. I. Pérez-Reyes would like to thank the support of CONACyT through its scholarship program.

Appendix A. Another approach with the Galerkin method

Here, another approach to the Galerkin method [38] is exposed. With this Galerkin method a more simple and tractable asymptotic approximation is available to the present eigenvalue problem. Due to the resulting magnitudes of (R,ω,k,Pr) (see Figs. 1 and 2), it was not possible to obtain asymptotic expressions for R and ω from the formula given in Eq. (16). Besides, the presence of $q=\sqrt{k^2+\sigma}$ in the argument of several hyperbolic functions makes it difficult to obtain asymptotic expansions.

Thus, the process to solve the eigenvalue problem posed in the system of Eqs. (9) and (10) subject to the boundary conditions Eq. (11) is to consider the following trial functions for W and Θ satisfying the boundary conditions Eq. (11),

$$W=\sum_{n=0}^{\infty}E_n[z(z-1)]^{2+n} \tag{A.1}$$

$$\Theta=G_0(1+Bz-Bz^2)+\sum_{n=1}^{\infty}G_n z^{n+1}\left(z-\frac{n+2+B}{n+1+B}\right) \tag{A.2}$$

After substitution of W and Θ given in Eqs. (A.1) and (A.2) in the system of Eqs. (9) and (10) the residuals are formed and they are made orthogonal to the respective trial functions

$$\begin{vmatrix} \int_0^1 W_m L_1 W n dz & -(1+F\sigma)Rk^2\int_0^1 W_m\Theta_n\,dz \\ \int_0^1 \Theta_m W_n\,dz & -\int_0^1 \Theta_m L_2\Theta_n\,dz \end{vmatrix}=0 \tag{A.3}$$

where the operators L_1 and L_2 are defined as

$$L_1=\frac{\sigma}{Pr}(1+F\sigma)\left(\frac{d^2}{dz^2}-k^2\right)-\left(\frac{d^2}{dz^2}-k^2\right)^2$$

$$L_2=\sigma-\left(\frac{d^2}{dz^2}-k^2\right)$$

Determinant Eq. (A.3) is a solvability condition from which R can be calculated. The first and second approximation of R can be easily calculated from the determinant Eq. (A.3) and although these are not presented here they can be obtained from the authors upon request. In the following sections these approximations are used to get asymptotic expressions for R and ω.

Appendix B. Asymptotics for $Pr\to\infty$

In this section asymptotic expressions were calculated for R and ω in the case of $Pr\to\infty$. Some ideas of Kolkka and Ierley [16] were used in the expansions of R and ω. Note that the formulas are large and complex because they include the conductivities ratio, not reported before for this viscoelastic problem.

As mentioned above two further approximations for the thicknesses ratio were made. These affect the hyperbolic function appearing in the Biot number. Thus for $D\to 0$ the Biot number is approximated as $B=(XD)^{-1}$ and for $D\to\infty$ it is $B=qX^{-1}$, respectively.

By using the first order approximation of the Galerkin method Eq. (A.3) some asymptotic expressions of R and ω were calculated.

B.1. Case of $Pr\to\infty$, $F\to 0$ and $D\to 0$

Here, use is made of the following expansion scheme

$$\omega^2=\omega_0^2Pr^{\frac{3}{2}}+\omega_1^2Pr+\omega_2^2Pr^{\frac{1}{2}}+O(1)$$

$$k=k_0Pr^{\frac{1}{4}}+O\left(Pr^{-\frac{3}{4}}\right)$$

and the resulting expressions are

$$\begin{aligned}R=C_5\Bigg[&\frac{C_6}{F^2}+\frac{1}{Fk_0^2\sqrt{Pr}}\Big[C_6Fk_0^4+14+320XD+2940X^2D^2\\&+12600X^3D^3+21600X^4D^4\Big]\\&+\frac{1}{Fk_0^4Pr}\Big[\left(22+400XD+2820X^2D^2+9000X^3D^3+10800X^4D^4\right)\\&\times Fk_0^4+C_6k_0^4+364+7440XD+62640X^2D^2\\&+259200X^3D^3+453600X^4D^4\Big]\Bigg]+O\left(\frac{1}{Pr^{\frac{3}{2}}}\right)\end{aligned}$$

$$\begin{aligned}\omega^2=\frac{1}{1+30X^2D^2+10XD}\Bigg[&C_6\frac{k_0^2Pr^{\frac{3}{2}}}{F}+(12F-1)C_6\frac{Pr}{F^2}\\&+\Big[360C_6F-2\left(1+40XD+540X^2D^2+2700X^3D^3+5400X^4D^4\right)\Big]\\&\times\frac{\sqrt{Pr}}{F^2k_0^2}-\Big[C_6\left(k_0^4+4320F\right)+340+6480XD+50400X^2D^2\\&+194400X^3D^3+324000X^4D^4\Big]\frac{1}{k_0^4F^2}\Bigg]+O\left(\frac{1}{\sqrt{Pr}}\right)\end{aligned}$$

B.2. Case of $Pr\to\infty$, $F\to 0$ and $D\to\infty$

Here, the expansion scheme was modified in order to include the effect of the conductivities ratio X as follows

$$\omega^2=\omega_0^2Pr+\omega_1^2Pr^{\frac{1}{2}}+\omega_2^2+O\left(Pr^{-\frac{1}{2}}\right)$$

$$k=k_0+O(Pr^{-1})$$

and the resulting expressions are

$$\begin{aligned}R=&\frac{1498}{675k_0^2F^{\frac{3}{2}}}\frac{\sqrt{k_0^4+24k_0^2+504}\sqrt{12+k_0^2}}{\sqrt{Pr}}\\&+\frac{2996X\sqrt{2}\left(k_0^6+36k_0^4+792k_0^2+6048\right)}{2025k_0^2\left(k_0^4+24k_0^2+504\right)^{\frac{3}{4}}\left(12+k_0^2\right)^{\frac{1}{4}}F^{\frac{5}{4}}Pr^{\frac{3}{4}}(1+X)}+O\left(\frac{1}{Pr}\right)\end{aligned}$$

$$\omega^2=\frac{\left(k_0^4+24k_0^2+504\right)Pr}{\left(12+k_0^2\right)F}-\sqrt{\frac{\left(k_0^4+24k_0^2+504\right)}{\left(12+k_0^2\right)F^3}}\sqrt{Pr}+O(1)$$

where C_5 and C_6 are coefficients that depend on the parameters (X,D), and are defined as follows

$$C_5=\frac{28}{3(3+14XD)^2(1+30X^2D^2+10XD)}$$

$$C_6=1+20XD+160X^2D^2+600X^3D^3+900X^4D^4$$

B.3. Case of $Pr \to \infty$, $F \to \infty$ and $D \to 0$

This case was calculated independently at a second order approximation with the Galerkin method Eq. (A.3). It is necessary to mention that the first order approximation is not good in this limit. For both cases $D \to 0$ and $D \to \infty$ it was considered first a two term expansion with respect to $Pr \to \infty$ and later the following expansion with respect to $F \to \infty$ was used

$$\omega^2 = \omega_0^2 F^{-1} + \omega_1^2 F^{-2} + O(F^{-3})$$
$$k = k_0 + O(F^{-1})$$

Thus, for $D \to 0$ we have

$$\begin{aligned}
R = C_7 \Bigg[& \left(X^2D^2 + \frac{XD}{3} + \frac{1}{30}\right)\left(5k_0^8 + 1056k_0^6 + 104544k_0^4 + 2471040k_0^2 + 40772160\right) \\
& \times \left[\frac{\left(3k_0^4 + 520k_0^2 + 40040\right)X^2D^2}{15} + \frac{\left(31k_0^4 + 5772k_0^2 + 463320\right)XD}{405} \times \frac{19k_0^4}{2430} + \frac{598k_0^2}{405} + \frac{16588}{135}\right] \\
& + \frac{1}{Pr}\left[\frac{k_0^2}{15}\left(15k_0^{10} + 5484k_0^8 + 949520k_0^6 + 86898240k_0^4 + 4063625280k_0^2 + 38869459200\right)X^4D^4 \right. \\
& + \left(\frac{58k_0^{12}}{81} + \frac{36608k_0^{10}}{135} + \frac{241608k_0^8}{5} + \frac{22600864k_0^6}{5} + 218366720k_0^4 + 2528477952k_0^2 + 5182594560\right)X^3D^3 \\
& + \left(\frac{k_0^{12}}{5} + \frac{157118k_0^{12}}{2025} + \frac{1909504k_0^8}{135} + \frac{12151568k_0^6}{9} + \frac{1008587008k_0^4}{15} + 905645312k_0^2 + 3109556736\right)X^2D^2 \\
& + \left(\frac{94k_0^{12}}{3645} + \frac{61864k_0^{10}}{6075} + \frac{1276984k_0^8}{675} + \frac{41371616k_0^6}{225} + \frac{141050624k_0^4}{15} + \frac{425641216k_0^2}{3} + 617723392\right)XD \\
& \left. + \frac{\left(k_0^2 + 10\right)}{72900}\left(95k_0^{10} + 36942k_0^8 + 6774768k_0^6 + 637034112k_0^4 + 30440494656k_0^2 + 295761248640\right)\right] + O\left(\frac{1}{Pr^2}\right)\Bigg]
\end{aligned}$$

$$\begin{aligned}
\omega^2 = & \left(5k_0^8 + 1056k_0^6 + 104544k_0^4 + 2471040k_0^2 + 40772160\right) \\
& \times \left[486\left(X^2D^2 + \frac{31XD}{81} + \frac{19}{486}\right)k_0^4 + 84240\left(X^2D^2 + \frac{37XD}{90} + \frac{23}{540}\right)k_0^2 + 6486480\left(X^2D^2 + \frac{3XD}{7} + \frac{29}{630}\right)\right]\left[\left(2430k_0^{10} + 888408k_0^8 \right.\right. \\
& + 153822240k_0^6 + 14077514880k_0^4 + 658307295360k_0^2 + 6296852390400)X^2D^2 + \left(930k_0^{10} + 357948k_0^8 + 64370592k_0^6 \right. \\
& \left.\left. + 5983870464k_0^4 + 283040334720k_0^2 + 2728636035840\right)XD + 95k^{10} + 36942k^8 + 6774768k^6 + 637034112k^4 \right. \\
& \left. + 30440494656k^2 + 295761248640\right]^{-1} Pr + O\left(Pr^2\right)
\end{aligned}$$

B.4. Case of $Pr \to \infty$, $F \to \infty$ and $D \to \infty$

Here, the expressions for $D \to \infty$ are

$$\begin{aligned}
R = C_8 \Big[& \left(5k_0^8 + 1056k_0^6 + 104544k_0^4 + 2471040k_0^2 + 40772160\right) \\
& \times \Big[\left(14580k_0^4 + 2527200k_0^2 + 194594400\right)k_0X^4 \\
& + \left(10080k_0^6 + 1797660k_0^4 + 141523200k_0^2 + 194594400\right)X^3 \\
& + \left(2832k_0^6 + 519660k_0^4 + 41614560k_0^2 + 64864800\right)k_0X^2 \\
& + \left(374k_0^6 + 70248k_0^4 + 5728320k_0^2 + 4942080\right)k_0^2X \\
& + \left(19k_0^4 + 3588k_0^2 + 298584\right)k_0^5\Big] \\
& + \left(30k_0X + 60X + 10k_0 + 10k_0^2X + k_0^3\right) \\
& \times \Big[\left(2430k_0^{10} + 888408k_0^8 + 153822240k_0^6 + 14077514880k_0^4 \right. \\
& + 658307295360k_0^2 + 6296852390400\Big)X^2 \\
& + \left(930k_0^{10} + 357948k_0^8 + 64370592k_0^6 + 5983870464k_0^4 \right. \\
& \left. + 283040334720k_0^2 + 2728636035840\right)k_0X \\
& + \left(95k_0^{10} + 36942k_0^8 + 6774768k_0^6 + 637034112k_0^4 \right. \\
& \left. + 30440494656k_0^2 + 295761248640\right)k_0^2\Big]\frac{1}{Pr} + O\left(\frac{1}{Pr^2}\right)\Big]
\end{aligned}$$

$$\begin{aligned}
\omega^2 = & \left(5k_0^8 + 1056k_0^6 + 104544k_0^4 + 2471040k_0^2 + 40772160\right) \\
& \times \left[19k_0^6 + 186k_0^5X + \left(3588 + 486X^2\right)k_0^4 + 34632Xk_0^3 + \left(298584 + 84240X^2\right)k_0^2 + 2779920Xk_0 + 6486480X^2\right] \\
& \times \left[95k_0^{12} + 930k_0^{11}X + \left(2430X^2 + 36942\right)k_0^{10} + 357948k_0^9X + \left(888408X^2 + 6774768\right)k_0^8 + 64370592k_0^7X \right. \\
& + \left(153822240X^2 + 637034112\right)k_0^6 + 5983870464k_0^5X + \left(14077514880X^2 + 30440494656\right)k_0^4 + 283040334720k_0^3X \\
& \left. + \left(658307295360X^2 + 295761248640\right)k_0^2 + 2728636035840Xk_0 + 6296852390400X^2\right]^{-1} Pr + O(Pr^2)
\end{aligned}$$

where C_7 and C_8 are coefficients that depend on the parameters (F, k_0, X, D), and are defined as follows

$$\begin{aligned}
C_7 = & \frac{350}{297k_0^2F}\left[\left(X^2D^2 + \frac{31XD}{81} + \frac{19}{486}\right)k_0^4 + \left(\frac{520X^2D^2}{30} + \frac{1924XD}{27} + \frac{598}{81}\right)k_0^2 \right. \\
& \left. + \frac{40040X^2D^2}{3} + 5720XD + \frac{16588}{27}\right]^{-2} \\
C_8 = & \frac{7}{433026k_0^3F}\left[\left(k_0^4 + \frac{520k_0^2}{3} + \frac{40040}{3}\right)X^2 + \frac{31}{81}\left(k_0^4 + \frac{5772k_0^2}{31} + \frac{463320}{31}\right)k_0X \right. \\
& \left. + \frac{19}{486}\left(k_0^4 + \frac{3588k_0^2}{19} + \frac{298584}{19}\right)\right]^{-2}
\end{aligned}$$

The asymptotic results of this appendix are in very good agreement with those of the numerical analysis.

Appendix C. Asymptotics for $F \to \infty$

In this limit, the second order Galerkin approximation Eq. (A.3) was necessary. Notice that the approximations presented in this appendix are valid for any Prandtl number. For both cases of $D \to 0$ and $D \to \infty$ the following expansion scheme for $F \to \infty$ was considered

$$\omega^2 = \omega_0^2 F^{-1} + \omega_1^2 F^{-2} + O(F^{-3})$$
$$k = k_0 + O(F^{-1})$$

C.1. Case for $D \to 0$

The expressions for any Prandtl number are

$$\begin{aligned}
R = C_{10}\Bigg[C_9\Bigg[&\Bigg(+\frac{254k_0^{12}}{10989}+\frac{41264k_0^{10}}{4995}+\frac{1666568k_0^8}{1665}+\frac{4735312}{111}k_0^6\\
&+\frac{9710272}{37}k_0^4-\frac{286256256}{37}k_0^2-\frac{5568076800}{37}\Bigg)X^2D^2\\
&\times\Bigg(\frac{347k_0^{12}}{32967}+\frac{58952k_0^{10}}{14985}+\frac{2536972k_0^8}{4995}+\frac{42840944k_0^6}{1665}\\
&+\frac{222100736k_0^4}{555}+\frac{38310272k_0^2}{37}-\frac{1540501248}{37}\Bigg)XD\\
&+\frac{659k_0^{12}}{593406}+\frac{19324k_0^{10}}{44955}+\frac{863234k_0^8}{14985}+\frac{5256808k_0^6}{1665}\\
&+\frac{35244352k_0^4}{555}+\frac{260438464k_0^2}{555}-\frac{89707904}{37}\Bigg]\\
&+\Bigg(k0^8+\frac{13456k_0^6}{37}+\frac{1400784k_0^4}{37}+\frac{25534080k_0^2}{37}+\frac{144555840}{37}\Bigg)\\
&\times\Bigg[\Bigg(k_0^8+\frac{1056k_0^6}{5}+\frac{235268k_0^4}{15}+471328k0^2+7673952\Bigg)X^2D^2\\
&+\Bigg(\frac{31k_0^8}{81}+\frac{10912k_0^6}{135}+\frac{254276k_0^4}{45}+\frac{2432144k_0^2}{15}+2914912\Bigg)XD\\
&+\frac{19k_0^8}{486}+\frac{3344k_0^6}{405}+\frac{74602k_0^4}{135}+\frac{129272k_0^2}{9}+\frac{1397968}{5}\Bigg]\Bigg]\frac{1}{F}+O\left(\frac{1}{F^2}\right)
\end{aligned}$$

$$\omega^2 = \frac{\left(5k_0^6+792k_0^4+52272k_0^2+617760-6C_9\right)Pr}{\left(5k_0^4+528k_0^2+5148\right)F}+O\left(\frac{1}{F^2}\right)$$

C.2. Case for $D \to \infty$

Here, for any Prandtl number, the solution is

$$\begin{aligned}
R = C_{11}\Bigg[C_9\Bigg[&\Bigg(\frac{254k_0^{12}}{10989}+\frac{41264k_0^{10}}{4995}+\frac{1666568k_0^8}{1665}+\frac{4735312k_0^6}{111}\\
&+\frac{9710272k_0^4}{37}-\frac{286256256k_0^2}{37}-\frac{5568076800}{37}\Bigg)X^2\\
&+\Bigg(\frac{347k_0^{13}}{32967}+\frac{58952k_0^{11}}{14985}+\frac{2536972k_0^9}{4995}+\frac{42840944k_0^7}{1665}\\
&+\frac{222100736k_0^5}{555}+\frac{38310272}{37}k_0^3-\frac{1540501248k_0}{37}\Bigg)X\\
&+\frac{659k_0^{14}}{593406}+\frac{19324}{44955}k_0^{12}+\frac{863234k_0^{10}}{14985}+\frac{5256808k_0^8}{1665}\\
&+\frac{35244352k_0^6}{555}+\frac{260438464k_0^4}{555}-\frac{89707904k_0^2}{37}\Bigg]\\
&+\Bigg(k_0^8+\frac{13456k_0^6}{37}+\frac{1400784k_0^4}{37}+\frac{25534080k_0^2}{37}+\frac{144555840}{37}\Bigg)\\
&\times\Bigg[\Bigg(k_0^8+\frac{1056k_0^6}{5}+\frac{235268k_0^4}{15}+471328k_0^2+7673952\Bigg)X^2\\
&+\Bigg(\frac{31k_0^9}{81}+\frac{10912k_0^7}{135}+\frac{254276k_0^5}{45}+\frac{2432144k_0^3}{15}+2914912k_0\Bigg)X\\
&+\frac{19k_0^{10}}{486}+\frac{3344k_0^8}{405}+\frac{74602k_0^6}{135}+\frac{129272k_0^4}{9}+\frac{1397968k_0^2}{5}\Bigg]\Bigg]\frac{1}{F}+O\left(\frac{1}{F^2}\right)
\end{aligned}$$

$$\omega^2 = \frac{\left(5k_0^6+792k_0^4+52272k_0^2+617760-6C_9\right)Pr}{\left(5k_0^4+528k_0^2+5148\right)F}+O\left(\frac{1}{F^2}\right)$$

where C_9, C_{10} and C_{11} are coefficients that depend on the parameters (Pr, k_0, X, D), and are defined as follows

$$C_9 = \sqrt{1221k_0^8+444048k_0^6+46225872k_0^4+842624640k_0^2+4770342720}$$

$$\begin{aligned}
C_{10} = 3398598000&\frac{\left[\left(X^2D^2+\frac{XD}{3}+\frac{1}{30}\right)k_0^2+2XD+\frac{1}{3}\right]\left(k_0^4+\frac{528k_0^2}{5}+\frac{5148}{5}\right)}{k_0^2Pr\left(5k_0^6+792k_0^4+52272k_0^2+617760-6C_9\right)}\\
&\times\Big[\left(13716X^2D^2+6246XD+659\right)k_0^6\\
&+\left(3441636X^2D^2+1617660XD+178530\right)k_0^4\\
&+486\left(C_9+\frac{1395680}{3}\right)X^2D^2k_0^2+(186C_9+104339664)XDk_0^2\\
&+(19C_9+11768328)k_0^2+42120(C_9+29172)X^2D^2\\
&+(17316C_9+602316000)XD+71474832+1794C_9\Big]^{-2}
\end{aligned}$$

$$\begin{aligned}
C_{11} = 3398598000&\frac{\left[\frac{k_0^3}{30}+\frac{k_0^2X}{3}+\left(\frac{1}{3}+X^2\right)k_0+2X\right]\left(k_0^4+\frac{528}{5}k_0^2+\frac{5148}{5}\right)}{k_0Pr\left(5k_0^6+792k_0^4+52272k_0^2+617760-6C9\right)}\\
&\times\Big[\left(13716k_0^6+3441636k_0^4+(226100160+486C_9)k_0^2\right.\\
&+1228724640+42120C_9)X^2\\
&+\left(6246k_0^7+1617660k_0^5+(186C_9+104339664)k_0^3\right.\\
&+(602316000+17316C9)k_0)X+659k_0^8+178530k_0^6\\
&+\left(11768328+19C_9)k_0^4+(71474832+1794C_9)k_0^2\right]^{-2}
\end{aligned}$$

The results given in this appendix agree very well with those of the numerical analysis.

References

[1] B.C. Bowen, B.H. Zimm, Molecular weight of T2 NaDNA from viscoelasticity, Biophys. Chem. 7 (1978) 235–252.
[2] P. Kolodner, Oscillatory convection in viscoelastic DNA suspensions, J. Non-Newtonian Fluid Mech. 75 (1998) 167–192.
[3] M. Krishnan, V.M. Ugaz, M.A. Burns, PCR in a Rayleigh–Bénard convection cell, Science 298 (2002) 793.
[4] D. Braun, A. Libchaber, Trapping of DNA by thermophoretic depletion and convection, Phys. Rev. Lett. 89 (2002) 188103.
[5] D. Braun, N.L. Goddard, A. Libchaber, Exponential DNA replication by laminar convection, Phys. Rev. Lett. 91 (2003) 158103.
[6] D. Braun, PCR by thermal convection, Mod. Phys. Lett. B 18 (2004) 775–784.
[7] C.B. Mast, D. Braun, Thermal trap for DNA replication, Phys. Rev. Lett. 104 (2010) 188102.
[8] C.V. Sri Krishna, Effects of non-inertial acceleration on the onset of convection in a second-order fluid-saturated porous medium, Int. J. Eng. Sci. 39 (2001) 599–609.

[9] D. Laroze, J. Martínez–Mardones, J. Bragard, C. Pérez–García, Realistic rotating convection in a DNA suspension, Physica A 385 (2007) 433–438.
[10] D. Laroze, J. Martínez–Mardones, J. Bragard, Thermal convection in a rotating binary viscoelastic liquid mixture, Eur. Phys. J.: Special Topics 146 (2007) 291–300.
[11] G.P. Metcalfe, R.P. Behringer, Critical Rayleigh numbers for cryogenic experiments, J. Low Temp. Phys. 78 (1990) 231–246.
[12] P. Cerisier, A. Rahal, J. Cordonnier, G. Lebon, Thermal influence of boundaries on the onset of Rayleigh–Bénard convection, Int. J. Heat Mass Transfer 41 (1998) 3309–3320.
[13] L.E. Howle, The effect of boundary properties on controlled Rayleigh–Bénard convection, J. Fluid Mech. 411 (2000) 39–58.
[14] C.M. Vest, V.S. Arpaci, Overstability of a viscoelastic fluid layer heated from below, J. Fluid Mech. 36 (1969) 613–623.
[15] M. Takashima, Thermal instability in a viscoelastic fluid layer. I, J. Phys. Soc. Jpn. 33 (1972) 511–518.
[16] R.W. Kolkka, G.R. Ierley, On the convected linear stability of a viscoelastic Oldroyd B fluid heated from below, J. Non–Newtonian Fluid Mech. 25 (1987) 209–237.
[17] J. Martínez–Mardones, C. Pérez–García, Linear instability in viscoelastic fluid convection, J. Phys.: Condens. Matter 2 (1990) 1281–1290.
[18] S. Rosenblat, Thermal convection in a viscoelastic liquid, J. Non-Newtonian Fluid Mech. 21 (1986) 201–223.
[19] H.M. Park, H.S. Lee, Nonlinear hydrodynamic stability of viscoelastic fluids heated from below, J. Non-Newtonian Fluid Mech. 60 (1995) 1–26.
[20] H.M. Park, H.S. Lee, Hopf bifurcations of viscoelastic fluids heated from below, J. Non-Newtonian Fluid Mech. 66 (1996) 1–34.
[21] J. Martínez–Mardones, R. Tiemann, D. Walgraef, W. Zeller, Amplitude equations and pattern selection in viscoelastic convection, Phys. Rev. E 54 (1996) 1478–1488.
[22] L.A. Dávalos-Orozco, E. Vázquez Luis, Natural convection of a viscoelastic fluid with deformable free surface, J. Non-Newtonian Fluid Mech. 85 (1999) 257–271.
[23] J. Martínez–Mardones, R. Tiemann, D. Walgraef, Convective and absolute instabilities in viscoelastic fluid convection, Physica A 268 (1999) 14–23.
[24] J. Martínez–Mardones, R. Tiemann, D. Walgraef, Rayleigh–Bénard convection in binary viscoelastic fluid, Physica A 283 (2000) 233–236.
[25] J. Martínez–Mardones, R. Tiemann, D. Walgraef, Convection in binary viscoelastic fluid, Rev. Mex. Fís. 44 (2002) 103–105.
[26] J. Martínez–Mardones, R. Tiemann, D. Walgraef, Amplitude equation for stationary convection in a binary viscoelastic fluid, Physica A 327 (2003) 29–33.
[27] Z. Li, R.E. Khayat, Three-dimensional thermal convection of viscoelastic fluids, Phys. Rev. E 71 (2005) 066305.
[28] P.C. Dauby, P. Parmentier, G. Lebon, M. Grmela, Coupled buoyancy and thermocapillary convection in a viscoelastic Maxwell fluid, J. Phys.: Condens. Matter 5 (1993) 4343–4352.
[29] G. Lebon, P. Parmentier, D. Teller, P.C. Dauby, Bénard–Marangoni instability in a viscoelastic jeffreys' fluid layer, Rheol. Acta 33 (1994) 257–266.
[30] P. Parmentier, G. Lebon, V. Regnier, Weakly nonlinear analysis of Bénard–Marangoni instanbility in viscoelastic fluids, J. Non-Newtonian Fluid Mech. 89 (2000) 63–95.
[31] D. Getachew, S. Rosenblat, Thermocapillary instability of a viscoelastic liquid layer, Acta Mech. 55 (1985) 137–149.
[32] S. Chandrasekhar, Hydrodynamic and Hydromagnetic Stability, Dover Publications, Inc., New York, NY, 1981.
[33] W.H. Press, S.A. Teukolsky, W.T. Vetteling, B.P. Flannery, Numerical Recipes, third ed., The Art of Scientific Computing, Cambridge University Press, Cambridge, 2007.
[34] M. Sokolov, R.I. Tanner, Convective instability of a general viscoelastic fluid heated from below, Phys. Fluids 15 (1972) 534–539.
[35] D.T.J. Hurle, E. Jakeman, E.R. Pike, On the solution of the Bénard problem with boundaries of finite conductivity, Proc. R. Soc. Lond. A 296 (1967) 469–475.
[36] L.A. Dávalos-Orozco, Magnetoconvection in a rotating fluid between walls of very low thermal conductivity, J. Phys. Soc. Jpn. 53 (1984) 2173–2176.
[37] L.A. Dávalos-Orozco, O. Manero, Thermoconvective instability of a second-order fluid, J. Phys. Soc. Jpn. 55 (1986) 442–445.
[38] B.A. Finlayson, The Method of Weighted Residuals and Variational Principles, Academic Press, Inc., New York, 1972.